Research Article
P-ISSN: 2971-785X, E-ISSN: 3141-4095
NIGERIAN JOURNAL OF ENGINEERING RESEARCH UNICROSS (NJERU)
DOI: 10.67571/njeru.2026.010108
Volume 3, Issue 1, 16 March 2026, 1-8

Minimizing Transient Voltage Excursions in DC-DC Boost Converters using Dual Loop Voltage-Current Control with Load Current Feed Forward (LCFF)

Peter O. Ohiero [a*]

[a] Department of Electrical and Electronic Engineering, Faculty of Engineering, University of Cross River State, Calabar, Nigeria.

[*]Corresponding author: peterohiero@unicross.edu.ng

Received: 13th November, 2025 Revised: 23rd January, 2026 Accepted: 8th February, 2026

ABSTRACT
Transient voltage excursions pose a significant challenge for DC-DC boost converters in high-dynamics applications, including electric vehicle power systems, renewable energy integration, and microgrids. Standard single-loop or dual-loop PI controllers frequently exhibit substantial voltage undershoot and prolonged recovery times, primarily due to the constraints of the Right-Half-Plane (RHP) zero inherent in boost converter topologies. To address these limitations, this paper presents an enhanced control strategy featuring a dual-loop voltage-current PI architecture integrated with a Load Current Feed-Forward (LCFF) mechanism. By bypassing the slower outer voltage loop, the LCFF branch enables an immediate duty cycle adjustment upon detecting load fluctuations. Simulation was carried out in MATLAB/Simulink using a 12–24 V boost converter under a 50% load step. Simulation results indicate that the proposed LCFF-based control significantly outperforms traditional dual-loop PI architectures, reducing peak voltage excursions by 72% and settling time by 52%.

Keywords*— Boost Converter, Transient Response, Dual-Loop Control, Load Current Feed Forward (LCFF), Voltage Excursion.*

I. INTRODUCTION

The DC-DC boost converter is a fundamental component in modern renewable-energy systems, electric vehicles and smart grids providing the necessary voltage step-up for battery-powered applications. However, the transient performance of the boost converter is limited by its non-minimum phase behaviour, where a sudden increase in load leads to an initial drop in output voltage before the controller can compensate [1][2].

Standard dual-loop control consisting of an outer voltage loop and an inner current loop improves stability but remains reactive rather than proactive. To minimize these voltage excursions, researchers have explored various techniques, including sliding mode control and model predictive control. However, these often require high computational power. This paper proposes Load Current Feed Forward (LCFF) as a computationally efficient method to achieve optimal transient recovery.

The transient voltage excursion of DC-DC boost converters under dynamic load conditions is a well-documented challenge in power electronics, primarily due to the non-minimum phase characteristics of the boost converter topology caused by the Right-Half

Plane (RHP) zero in the control-to-output transfer function.

Early research into boost converter regulation relied heavily on single-loop voltage non-linear and intelligent control paradigms such as Sliding Mode Control (SMC), Model Predictive Control (MPC), and Fuzzy Logic [3][4][5]. While these methods offer high performance, their industrial adoption is often hindered by complexity, hardware costs and other limitations. However, several studies [6][7] noted that single-loop architectures often fail to provide sufficient stability during high-frequency load switching. The introduction of dual-loop control consisting of an inner current loop and an outer voltage loop became the industrial standard [8][9]. This architecture improves the dynamic response by providing active current limiting and better damping.

Despite these improvements, traditional dual-loop PI controllers are inherently reactive. Research conducted between 2020 and 2024 [10][11] highlighted that the presence of a Right-Half-Plane (RHP) zero in the boost converter's transfer function severely limits the achievable bandwidth of the voltage loop. When a sudden load step occurs, the controller cannot immediately increase the duty cycle without causing an initial transient dip, leading to significant voltage excursions. Recent advancements have sought to mitigate this using adaptive neural network-based fractional-order proportional integrated derivative controller. Abdollahzadeh et al. [12] explored combining adaptive neural network with Fractional order Proportional Integrated Derivative (FOPID) fractional order PI controllers. The primary disadvantages of an adaptive neural network-based fractional order proportional-integrated derivative (ANNC-FOPID) controller on a DC/DC Boost converter are high computational burden, implementation complexity, and potential slower dynamics in practical, fast-switching applications.

This paper has presented an enhanced control strategy for minimizing transient voltage excursions in DC-DC boost converters by integrating a linearized Load Current Feed-Forward (LCFF) into a traditional dual-loop Voltage-Current Control (VCC) architecture that maintains stability across a wide operating range without requiring high computational non-linear solvers.

The fundamental novelty of the Dual-Loop LCFF over traditional feed-forward methods lies in shifting feed-forward from a simple duty cycle boost to an instantaneous power-balancing current reference driver. By feeding the load disturbance into the high-bandwidth inner current loop rather than the PWM stage or voltage loop, it bypasses the voltage loop lag without triggering the destructive transient undershoot associated with the boost converter's Right Half-Plane zero. By sensing load current directly, the controller commands an increase in inductor current at the exact moment the load changes. While the RHP zero still exists physically, the surprise element of the disturbance is removed. The LCFF acts on the inner current loop, which has a much higher bandwidth than the outer voltage loop. Because the current loop does not see the RHP zero which is a property of the output voltage, it can respond with extreme speed to satisfy the new power demand. Since the LCFF is a feed-forward path and not part of the closed-loop characteristic equation, it allows for a more aggressive transient response without pushing the system toward the instability region typically associated with RHP zeros.

Table I shows the comparison of the different control strategies for DC – DC converter. The proposed LCFF integrated controller is linear and proactive, low computational cost, moderate design complexity and mitigate RHP Zero Impact.

TABLE I

COMPARISON OF CONTROL STRATEGIES FOR DC -DC CONVERTER

Feature	Traditional PI	SMC/MPC/ ANNC	Proposed LCFF
Response Type	Reactive	Proactive (Non-linear)	Proactive (Linear)

Computational Cost	Low	High	Low
Design Complexity	Simple	Complex	Moderate
RHP Zero Impact	High	Managed	Mitigated

II. Mathematical Modelling

The performance of the proposed control strategy depends on an accurate representation of the boost converter dynamics and the integration of the feed-forward path into the dual-loop structure.

A. Dynamic State Equations

Consider an ideal continuous conduction mode (CCM) boost converter in Figure 1 operating with Input voltage (V_{in}), Inductor (L) (with current i_L), Output Capacitor C_2 (with voltage v_{c2}), Load resistor R_L, and Duty cycle d [13].

Assume ideal switches and negligible parasitic resistances for brevity and given the state vector $\mathbf{x}(t) = \begin{bmatrix} i_L(t) \\ v_{c_2}(t) \end{bmatrix}$ and input vector $u(t) = v_{in}(t)$.

At State 1, when the Switch is ON ($0 < t \leq d \cdot T_s$), The inductor charges from V_{in}, while the capacitor discharges through R_L given by:

$$\frac{di_L}{dt} = \frac{1}{L} v_{in} \quad (1)$$

$$\frac{dv_{c_2}}{dt} = -\frac{1}{R_L C_2} v_{c_2} \quad (2)$$

This can be represented in Matrix form (A_1, B_1) as:

$$\begin{bmatrix} \frac{di_L}{dt} \\ \frac{dv_{c_2}}{dt} \end{bmatrix} = \begin{bmatrix} 0 & 0 \\ 0 & -\frac{1}{R_L C_2} \end{bmatrix} \begin{bmatrix} i_L \\ v_{c_2} \end{bmatrix} + \begin{bmatrix} \frac{1}{L} \\ 0 \end{bmatrix} v_{in} \quad (3)$$

At State 2, when the Switch is OFF ($d \cdot T_s < t \leq T_s$), the inductor discharges into the capacitor and load for interval duration of $d' = 1 - d$):

$$\frac{di_L}{dt} = \frac{1}{L} v_{in} - \frac{1}{L} v_{c_2} \quad (4)$$

$$\frac{dv_c}{dt} = \frac{1}{C_2} i_L - \frac{1}{R_L C} v_{c_2} \quad (5)$$

Equations (4) and (5) can be represented in Matrix form (A_2, B_2) as:

$$\begin{bmatrix} \frac{di_L}{dt} \\ \frac{dv_{c_2}}{dt} \end{bmatrix} = \begin{bmatrix} 0 & -\frac{1}{L} \\ \frac{1}{C_2} & -\frac{1}{R_L C_2} \end{bmatrix} \begin{bmatrix} i_L \\ v_{c_2} \end{bmatrix} + \begin{bmatrix} \frac{1}{L} \\ 0 \end{bmatrix} v_{in} \quad (6)$$

B. State-Space Averaging

Weighting the system matrices by d and $d' = 1 - d$:

$$A = dA_1 + (1 - d)A_2 = \begin{bmatrix} 0 & -\frac{1-d}{L} \\ \frac{1-d}{C_2} & -\frac{1}{R_L C_2} \end{bmatrix} \quad (7)$$

$$B = dB_1 + (1 - d)B_2 = \begin{bmatrix} \frac{1}{L} \\ 0 \end{bmatrix} \quad (8)$$

This yields the averaged continuous-time state equations:

$$\frac{d\bar{\imath}_L}{dt} = \frac{1}{L} \bar{v}_{in} - \frac{1-d}{L} \bar{v}_{C_2} \quad (9)$$

$$\frac{d\bar{v}_C}{dt} = \frac{1-d}{C_2} \bar{\imath}_L - \frac{1}{R_L C_2} \bar{v}_{C_2} \quad (10)$$

C. Perturbation and Linearization

Introduce small AC perturbations around the steady-state DC operating point (I_L, V_{C_2}, V_{in}, D):

$$\bar{\imath}_L = I_L + \hat{\imath}_L \quad (11)$$

$$\bar{v}_c = V_{C_2} + \hat{v}_{C_2} \quad (12)$$

$$\bar{v}_{in} = V_{in} + \hat{v}_{in} \quad (13)$$

$d = D + \hat{d}$ (and $1 - d = D' - \hat{d}$, where $D' = 1 - D$)

Substituting these into the averaged equations and removing DC terms and 2nd-order non-linear products (e.g., $\hat{d} \cdot \hat{v}_{C_2} \approx 0$):

D. Small-Signal AC State Equations:

Classical state-space averaging provides the small-signal transfer function $G_{vd}(s)$ for peak current-mode converters. However, when high-frequency dynamics near half the switching frequency are critical, extended describing functions yield higher fidelity.

$$\frac{d\hat{\imath}_L}{dt} = \frac{1}{L} \hat{v}_{in} - \frac{D'}{L} \hat{v}_{C_2} + \frac{V_{C_2}}{L} \hat{d} \quad (14)$$

$$\frac{d\hat{v}_{C_2}}{dt} = \frac{D'}{C_2} \hat{\imath}_L - \frac{1}{R_L C_2} \hat{v}_{C_2} - \frac{I_L}{C_2} \hat{d} \quad (15)$$

Note that DC relations are given as $V_{C_2} = \frac{V_{in}}{D'} = \frac{V_{in}}{1-D}$ and $I_L = \frac{V_{C_2}}{D' R_L} = \frac{V_{in}}{D'^2 R_L}$.

E. Control-to-Output Transfer Function $G_{vd}(s)$

To find $G_{vd}(s) = \frac{\hat{v}_o(s)}{\hat{d}(s)}$, set input voltage perturbation to zero ($\hat{v}_{in} = 0$) and transform to the Laplace domain (s) as follows:

From the inductor equation:

$$sL\hat{\imath}_L(s) = -D'\hat{v}_{C_2}(s) + V_{C_2}\hat{d}(s) \Rightarrow \hat{\imath}_L(s) = \frac{V_{C_2}\hat{d}(s) - D'\hat{v}_{C_2}(s)}{sL} \quad (16)$$

Substitute $\hat{\imath}_L(s)$into the capacitor equation:

$$sC\hat{v}_{C_2}(s) = \frac{D'}{sL}\left(V_{C_2}\hat{d}(s) - D'\hat{v}_{C_2}(s)\right) - \frac{\hat{v}_{C_2}(s)}{R_L} - I_L\hat{d}(s) \quad (17)$$

Grouping $\hat{v}_{C_2}(s)$terms:

$$\hat{v}_{C_2}(s)\left[sC_2 + \frac{1}{R_L} + \frac{D'^2}{sL}\right] = \hat{d}(s)\left[\frac{D'V_{C_2}}{sL} - I_L\right] \quad (18)$$

Multiplying through by sL and substituting $I_L = \frac{V_{C_2}}{D'R_L}$:

$$\hat{v}_{C_2}(s)\left[s^2LC_2 + s\frac{L}{R_L} + D'^2\right] = \hat{d}(s)\left[D'V_{C_2} - sL\frac{V_{C_2}}{D'R_L}\right] \quad (19)$$

Dividing by D'^2:

$$G_{vd}(s) = \frac{\hat{v}_o(s)}{\hat{d}(s)} = \frac{V_{C_2}}{D'} \cdot \frac{1 - s\frac{L}{D'^2R_L}}{1 + s\frac{L}{D'^2R_L} + s^2\frac{LC_2}{D'^2}} \quad (20)$$

$$G_{vd}(s) = \frac{\hat{v}_o(s)}{\hat{d}(s)} = \frac{V_{in}}{(1-D)^2} \cdot \frac{1 - s\frac{L}{(1-D)^2R_L}}{1 + s\frac{L}{(1-D)^2R_L} + s^2\frac{LC_2}{(1-D)^2}} \quad (21)$$

A critical observation in this model is the Right-Half-Plane (RHP) Zero at $z_{rhp} = \frac{R(1-D)^2}{R}$. This zero, limits the bandwidth of the outer voltage loop, as an increase in D initially causes V_o to drop before increasing, creating the transient excursion problem.

F. Proposed Control Strategy

The proposed system uses a nested loop structure consisting of the Inner Current Loop, the Outer Voltage Loop and the Load Current Feed Forward Path. The Inner Current Loop regulates the inductor current for high-speed protection while the Outer Voltage Loop maintains the output voltage at the reference and the LCFF Path injects the sensed load current directly into the current reference.

The Load Current Feed Forward Mechanism:

The load current acts as a primary disturbance. The objective of LCFF is to compensate for the load current disturbance Δi_o immediately. The output capacitor current is defined by:

$$i_C = C\frac{dv_o}{dt} = (1-D)i_L - i_o \quad (22)$$

Under a load step change Δi_o, the output voltage excursion Δv_o is minimized if the inductor current i_L is adjusted instantaneously. To maintain $\frac{dv_o}{dt} = 0$, the required change in inductor current Δi_L is;

$$\Delta i_L = \frac{1}{1-D}\Delta i_O \quad (23)$$

Where: K_{ff} is the feed -forward gain, ideally calculated as ${}^{1}/_{(1-D)}$.

By injecting $K_{ff}i_O$ directly into the current reference i_{ref}, the inner loop ramps up the inductor current as soon as the load sensor detects a change, bypassing the delay inherent in the voltage compensator of the outer loop.

Stability Analysis:

In a standard PI controller, the error must manifest before the controller reacts. With LCFF, the current reference is modified as:

$$i_{ref} = G_v(s)\left(V_{ref} - v_o\right) + K_{ff}i_o \quad (24)$$

Stability is ensured by selecting $G_v(s)$ such that the phase margin remains above 45^0 despite the injection of the feed forward signal. Since K_{ff} is a static gain derived from the steady-state duty cycle D, it does not introduce a new pole, preserving the original stability margins of the dual loop system while significantly improving disturbance rejection.

III. Modelling And Simulation of DC – DC Converter and Control

Figure 1 shows the equivalent circuit of a DC – DC Boost converter with the proposed load current feed forward control technique aimed at minimizing the voltage excursion of a DC – DC boost converter.

A DC-DC boost converter, often called a step-up converter, is a power electronics circuit that increases a lower input DC voltage to a higher output DC voltage. It is a class of Switched-Mode Power Supply (SMPS).

A standard boost converter consists of five primary components which includes Inductor (L), Switching Device (Q1), Diode (D), Output Capacitor (C) and Controller. The inductor stores energy in its magnetic field when the switch is closed while the switching device (Q1) usually a MOSFET or IGBT, toggles between ON and OFF states at high frequencies (typically 20 kHz to several MHz). The Diode (D) ensures that current flows only toward the load and prevents the capacitor from discharging back through the switch. The output capacitor (C) smooths the output voltage and provides power to the load when the inductor is charging. And the controller regulates the output by adjusting the duty cycle (D).

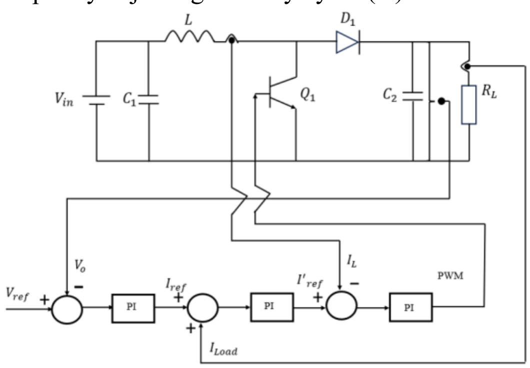

FIGURE 1: A DC – DC BOOST CONVERTER WITH LOAD CURRENT FEED FORWARD CONTROL TECHNIQUE

TABLE II

PARAMETERS OF THE DC -DC CONVERTER

Component	Typical Value
Input Voltage (Vin)	12V
Output Voltage (Vo)	24V
Inductor (L)	100uH with 20mΩ series resistor
Output Cap (C)	1000uF
Switching Freq (fsw)	50 kHz - 200 kHz

The system is modelled in MATLAB/Simulink with the control structure modelled in a hierarchical manner where the feed-forward path bypasses the inherent delays of the feedback loops using the parameters in Table II.

IV. RESULTS AND DISCUSSIONS

To verify the performance of the DC – DC Boost Converter with the dual-loop load current feed forward, a dynamic model is developed and simulated in MATLAB/Simulink as shown in Figure 2. The control is implemented using a standard Proportional Integral (PI) control. Two resistors R1 of 15Ω ohms and R2 of 30 Ω are connected in parallel to represent the load resistance. R2 is connected through a circuit breaker which was set to close at the time 0.25s to enable the load resistance to switch from 15Ω to 10Ω increasing the load from 1.6A to 2.4A. The simulation was conducted for standard dual-loop PI control and standard dual-loop PI with LCFF control techniques each for 0.5s.

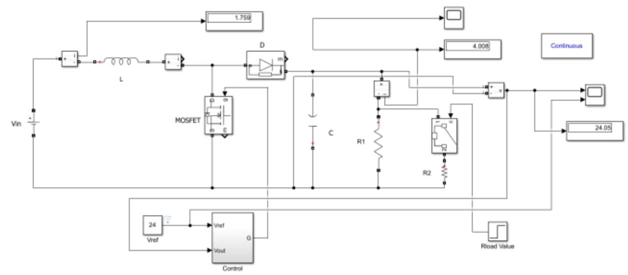

FIGURE. 2. DC – DC BOOST CONVERTER MODEL WITH LCFF IN MATLAB/SIMULINK

At first, simulation was conducted for standard dual-loop PI control technique. The load resistance changed from 15Ω to 10Ω at 0.25s causing the load current to change from 1.6A to 2.4A causing a transient event with a voltage undershoot with a longer settling time as shown in Figure 3 and a zoomed section of the voltage excursion shown in Figure 4.

At the second instant, simulation was conducted for the proposed standard dual-loop PI with LCFF control technique. Again, the load resistance is changed from 15Ω to 10Ω at 0.25s causing load current to settles with low settling time with a transient event with a voltage undershoot as shown in Figure 5 and a zoomed section of the voltage excursion shown in Figure 6.

The performance of the proposed dual-loop PI control with LCFF is evaluated against the conventional standard dual-loop PI control. As shown in Figure 3 and Figure 4, a load step from 1.6A to 2.4A at t = 0.25s causes a significant voltage excursion (deep undershoot) in the standard dual loop PI controller. This is due to the controller's inability to immediately account for the increased load demand before the outer voltage loop registers a significant error. When the load increases, the capacitor discharges rapidly, causing a significant undershoot. The voltage loop must wait for this error to build up before increasing the current reference. This causes a slow recovery because the PI controller's integral term must accumulate the error before the inductor current rises. The inductor current ramps up slowly with a visible lag relative to the load change.

Figure 5 and Figure 6 shows output voltage of the proposed dual loop PI with LCFF control technique. In contrast to the dual loop PI controller, the LCFF integrated controller anticipates the energy deficit by directly injecting the load current measurement (iload) shown in Figure 7 into the output of the voltage controller (the current loop's reference), bypasses the slower outer voltage loop and increasing the duty cycle as shown in Figure 8, leading to reduced voltage undershoot with a low settling time. Table III shows the comparison of the transient performance between the dual loop PI control and the dual loop PI with LCFF control. The comparison focuses on the transient recovery of the output voltage (Vo) following a 50% step-load increase as seen in Figure 4 and Figure 6.

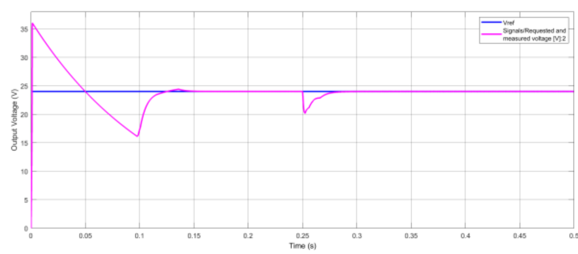

FIGURE 3: OUTPUT VOLTAGE WITH DUAL LOOP PI CONTROL ONLY WHEN THE LOAD RESISTANCE CHANGES FROM 15Ω TO 10Ω.

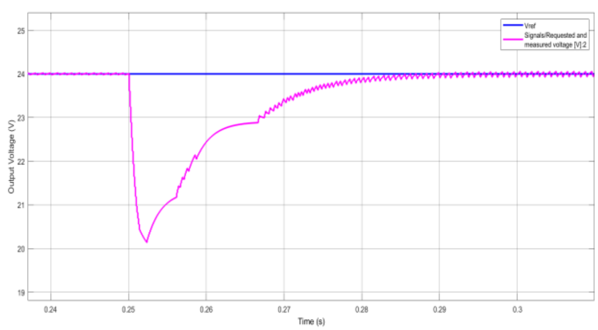

FIGURE 4: OUTPUT VOLTAGE WITH DUAL LOOP PI CONTROL ONLY SHOWING A ZOOMED SECTION OF THE TRANSIENT VOLTAGE EXCURSION/UNDERSHOOT WHEN THE LOAD RESISTANCE CHANGES FROM 15Ω TO 10Ω

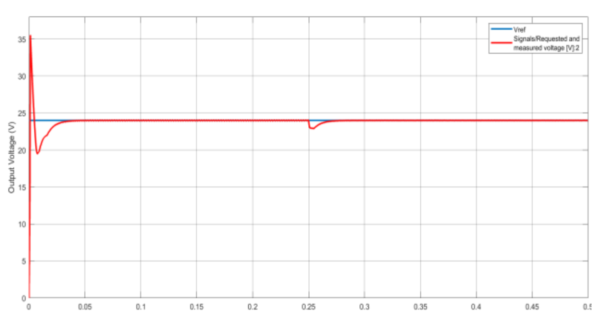

FIGURE 5: OUTPUT VOLTAGE WITH DUAL LOOP PI WITH LCFF CONTROL WHEN THE LOAD RESISTANCE CHANGES FROM 15Ω TO 10Ω.

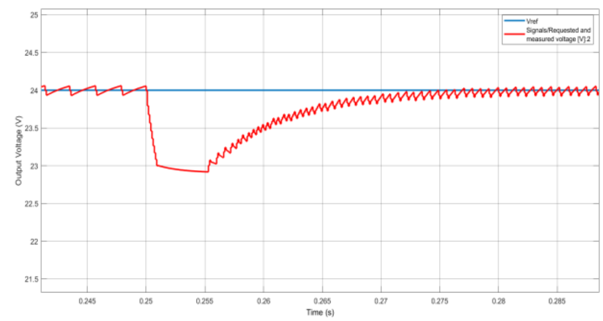

FIGURE 6: OUTPUT VOLTAGE WITH DUAL LOOP PI WITH LCFF CONTROL SHOWING A ZOOMED SECTION OF THE TRANSIENT VOLTAGE EXCURSION/UNDERSHOOT WHEN THE LOAD RESISTANCE CHANGES FROM 15Ω TO 10Ω.

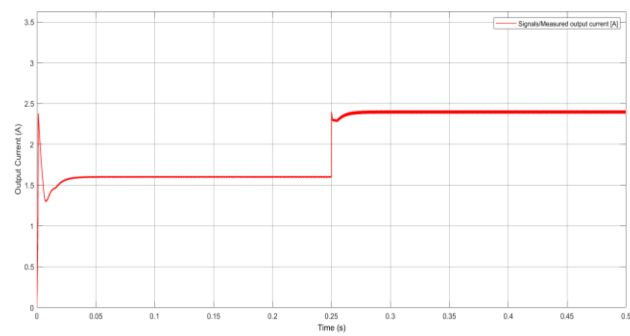

FIGURE 7 OUTPUT CURRENT OF DUAL LOOP PI WITH LCFF WHEN THE LOAD RESISTANCE CHANGES FROM 15Ω TO 10Ω.

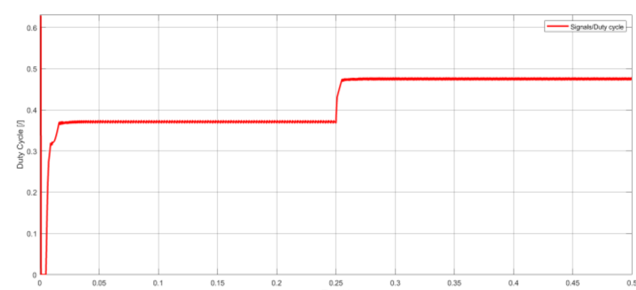

FIGURE 8. DUTY CYCLE OF DUAL LOOP PI WITH LCFF WHEN THE LOAD RESISTANCE CHANGES FROM 15Ω TO 10Ω.

The LCFF integrated controller has a reduced voltage undershoot of 1.1V and a shorter settling time of 0.024s compared to the voltage undershoot of 3.9V and a settling time of 0.05s recorded by standard dual loop PI controller. The proposed dual loop PI with LCFF control shows a superior performance with voltage undershoot improvement of 72% and a settling time improvement of 52% over the standard dual loop PI control.

TABLE III

COMPARISON OF TRANSIENT PERFORMANCE OF THE STANDARD DUAL-LOOP PI AND STANDARD DUAL-LOOP INTEGRATED WITH LCFF WITH A STEPPED-UP LOAD (50% STEPPED UP LOAD)

Metric	PI Control	Proposed PI with LCFF Control	Improvement (%)
Voltage Undershoot (V)	3.9	1.1	72
Settling Time (s)	0.05	0.024	52

V. CONCLUSIONS

This paper has presented an enhanced control strategy for minimizing transient voltage excursions in DC-DC boost converters by integrating Load Current Feed Forward (LCFF) into a traditional dual-loop PI control architecture. Integrating LCFF into a dual-loop boost converter transforms the control from reactive to proactive. By bypassing the slow voltage loop for load disturbances, LCFF decouples the load disturbance from the voltage loop error, allowing the current loop to handle the bulk of the transient, minimizes transient excursions, improve power quality, maintains high-frequency stability despite the narrow bandwidth of the voltage loop and potentially reduce the physical size and cost of the output filter capacitor. Because the feed-forward path is essentially an algebraic addition, it does not introduce new poles that would reduce the phase margin. This allows the converter to handle high-frequency load switching (up to 20 kHz) without the chattering or cumulative voltage drift often seen in single-loop or pure feedback architectures.

The simulation results confirmed a 72% reduction in voltage undershoot and a 52% improvement in settling time compared to standard dual loop PI control. The proposed method maintains linear stability margins, provides a robust, low-latency response to load disturbances making it safer for industrial deployment than heuristic or non-linear methods like Fuzzy Logic or SMC.

While adding a current sensor increases cost, the downsizing of the output capacitor as less storage is needed to cover the dip, offsets this expense.

AI DISCLOSURE STATEMENT.

This is to acknowledge that the Author(s) did not use any AI tool in the cause of this research.

References

[1] Y. El Haj, A. Sheir, R. Milman and V. K. Sood, "Robust Integral Sliding Mode Control of Non-minimum Phase DC-DC Converters," 2020 IEEE Electric Power and Energy Conference (EPEC), Edmonton, AB, Canada, 2020, pp. 1-7, Doi: 10.1109/EPEC48502.2020.9320126.

[2] Kalvapalli, Srikanth Reddy, R. Jeyasenthil, Tarakanath Kobaku, and Vivek Agarwal. "QFT Based Robust Tracking Control of Non-Minimum Phase Boost DC-DC Converter with Sensor Noise Suppression." *IEEE Transactions on Power Electronics* (2025),1-5, 10.1109/TPEL.2025.3527020

[3] P. Kumar and M. Ajmeri, "Comparison of Control Techniques for a DC-DC Boost Converter Exhibiting Non-minimum Phase Behaviour," 2022 2nd International Conference on Emerging Frontiers in Electrical and Electronic Technologies (ICEFEET), Patna, India, 2022, pp. 1-6, doi: 10.1109/ICEFEET51821.2022.9848100.

[4] B. Yadav and S. KV, "Model Predictive Control of Non-Minimum Phase DC-DC Boost Converter," 2023 5th International Conference on Energy, Power and Environment: Towards Flexible Green Energy Technologies (ICEPE), Shillong, India, 2023, pp. 1-6, doi: 10.1109/ICEPE57949.2023.10201649.

[5] E. Garza-Arias, J. C. Mayo-Maldonado, J. E. Valdez-Resendiz, G. Escobar, J. C. Rosas-Caro and D. Guillen, "Direct Output-Voltage Control of Nonminimum Phase Higher Order DC–DC Converters," in IEEE Transactions on Industrial Electronics, vol. 70, no. 2, pp. 1455-1466, Feb. 2023, doi: 10.1109/TIE.2022.3157984).

[6] El Aroudi, Abdelali, Reham Haroun, Mohammed S. Al-Numay, Javier Calvente, and Roberto Giral. "Fast-scale stability analysis of a DC–DC boost converter with a constant power load." *IEEE Journal of Emerging and Selected Topics in Power Electronics* 9, no. 1 (2019): 549-558.

[7] S. -K. Kim and C. K. Ahn, "Proportional-Derivative Voltage Control with Active Damping for DC/DC Boost Converters via Current Sensorless Approach," in IEEE Transactions on Circuits and Systems II: Express Briefs, vol. 68,

no. 2, pp. 737-741, Feb. 2021, doi: 10.1109/TCSII.2020.3008432.

[8] Özdemir, Ayhan, and Zekiye Erdem. "Double-loop PI controller design of the DC-DC boost converter with a proposed approach for calculation of the controller parameters." Proceedings of the Institution of Mechanical Engineers, Part I: Journal of Systems and Control Engineering 232, no. 2 (2018): 137-148.

[9] Asma, Charaabi, Zaidi Abdelaziz, and Zanzouri Nadia. "Dual loop control of DC-DC boost converter based cascade sliding mode control." In *2017 International Conference on Green Energy Conversion Systems (GECS)*, pp. 1-6. IEEE, 2017.

[10] S. Sarkar and S. S. Ghosh, "Comparison of Different Types of Internal Model Controller architecture for a Boost Converter," 2020 IEEE International Conference on Power Electronics, Smart Grid and Renewable Energy (PESGRE2020), Cochin, India, 2020, pp. 1-6, doi: 10.1109/PESGRE45664.2020.9070368.

[11] P. Verma and M. N. Anwar, "Control of Boost Converter using Internal Model Control scheme in single loop and in cascade control structure," 2021 IEEE 18th India Council International Conference (INDICON), Guwahati, India, 2021, pp. 1-6, doi: 10.1109/INDICON52576.2021.9691556.

[12] Mohammad Abdollahzadeh, Hasan Mollaee, Seyyed Morteza Ghamari, Fatemeh Khavari, “Design of a novel robust adaptive neural network-based fractional-order proportional-integrated-derivative controller on DC/DC Boost converter”, J. Eng. 2023; 2023: e12255. wileyonlinelibrary.com/iet-joe, DOI: 10.1049/tje2.12255, pp 1 – 13.

[13] J. G. Parada Salado, C. A. Herrera Ramírez, A. G. Soriano Sánchez, and M. A. Rodríguez Licea, "Nonlinear Stabilization Controller for the Boost Converter with a Constant Power Load in Both Continuous and Discontinuous Conduction Modes," *Micromachines*, vol. 12, no. 5, p. 522, May 2021. Doi: 10.3390/mi12050522.